

Application Note #203

Utilizing Nanoscale IR Spectroscopy to Characterize Biological Samples in Nanoscale Detail

The combination of atomic force microscopy (AFM) with infrared spectroscopy (IR) techniques, known as AFM-IR, allows for the chemical characterization of samples in nanoscale detail that would not be possible with the two techniques alone. AFM-IR spectroscopy, or nanoscale IR spectroscopy, has many applications including polymer characterization, pharmaceutical science, microelectronics, and life sciences. This application note introduces the principles and advancements of AFM-IR and provides examples of AFM-IR applications in the life sciences, specifically for the nanoscale characterization of biological samples including proteins, structures within single cells, monolayers, and tissues.

Principles and advancements of photothermal AFM-IR

Infrared (IR) spectroscopy is one of the most recognized analytical techniques for chemical analysis and characterization of materials by academic, government, and industrial R&D laboratories. Although conventional bulk IR spectroscopy is useful for many applications, it is constrained to a diffraction limit of 3 to 10 μm . Atomic force microscopy (AFM) is a widely used nanoscale imaging technique that provides users with a topographic map of a sample surface with high spatial resolution, approximately 1 nm laterally. While AFM is useful for visualizing the surface of a material, it cannot chemically characterize the material of interest. However, when combined with

an IR source, the resulting AFM-IR technique breaks the diffraction limit of conventional IR spectroscopy by orders of magnitude and provides the high-resolution imaging capabilities of AFM, while allowing for the chemical analysis of the material by the IR spectrophotometer.^{1,2}

The photothermal AFM-IR systems works by first illuminating the sample with a pulsed tunable IR laser. If the wavenumber of the laser source is in resonance with a molecular vibrational frequency in the sample, the IR radiation can be absorbed. When the molecules return to their ground vibrational state after exchanging energy with the sample matrix, the sample thermally expands over an area corresponding to the focused IR laser spot. The local thermal expansion of the material in proximity to the tip of the AFM probe causes the cantilever to oscillate. The oscillation is proportional to the radiation absorbed by the sample, so as the cantilever and tip move across a sample, both chemical images and topographical data are collected in nanoscale detail.

In the initial configuration of photothermal AFM-IR, the optical parametric oscillator (OPO) tunable laser source had a repetition rate of 1 kHz and a pulse length of ~ 10 ns, resulting in a rapid expansion of the sample inducing an impulse in the cantilever. This would cause the cantilever oscillation to ring down at its natural resonance frequencies after each laser pulse. A more recent advancement of photothermal AFM-IR replaces the OPO tunable laser source with a variable repetition rate quantum cascade

laser (QCL), resulting in an photothermal AFM-IR signal enhancement by two orders of magnitude (Figure 1). This enhancement is accomplished by tuning the QCL repetition rate to match the contact resonant frequency mode of the AFM cantilever.^{3,4} At the contact resonance, the oscillation amplitude of the cantilever is significantly increased relative to off-resonance frequencies. The AFM-IR signal can be further enhanced when a gold-coated AFM tip is used, producing a “lightning rod” effect that localizes the electric field at the tip apex. The combination of matching the repetition rate of the laser to the contact resonance of the AFM cantilever and using a gold-coated probe allows for the collection of IR spectra of samples down to ~10 nm in thickness. If the thin film sample is deposited onto a gold substrate, a further increase in the local enhancement of the electric field allows measurements down to 1 nm. Thus, when operated in resonance-enhanced mode, the photothermal AFM-IR technique can detect monolayer coverages of material on metal surfaces at lateral spatial resolutions down to 25x25 nm.

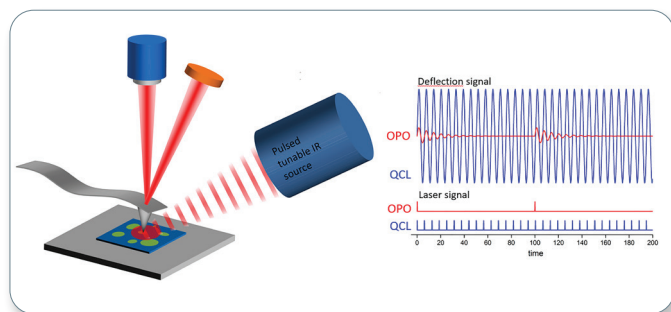


Figure 1. Optical diagram of an AFM-IR experiment showing the difference between the signal responses using a 1-kHz repetition rate OPO laser source and a QCL source with its repetition rate tuned to a contact resonance frequency mode of the AFM cantilever. Adapted from Marcott et al.⁵

Examples of AFM-IR applications for characterizing biological samples

AFM-IR has been used to characterize a variety of biological samples and answer a multitude of research questions in the life sciences. Examples of the nanoscale characterization of biological samples including proteins, structures within single cells, monolayers, and tissues are provided below. These findings would not be possible without the utilization of AFM-IR techniques.

Detection of photocycle branching of bacteriorhodopsin molecules embedded in purple membrane on a gold-coated substrate

In a study by Giliberti et al., AFM-IR was used to investigate the light-induced conformational changes of a bacteriorhodopsin (BR) mutant within patches of the purple membrane of *Halobacterium halobium*, a light-harvesting microorganism.⁶ BR is a photosensitive protein that acts as a proton pump, moving protons across the membrane

and subsequently converting light into chemical energy. The conformational changes that occur in the light-sensitive protein and its cofactor are the basis of their physiological functions. AFM and IR spectroscopy techniques alone are not sufficient to investigate questions about this system as relates to chemical characteristics in nanoscale detail. AFM is useful for detection of electric currents through protein monolayers, but not conformational changes in proteins. Traditional IR spectroscopy could be used to track conformational changes, although the sample is typically a liquid suspension or thick film with a high volume of purified protein.

By using AFM-IR, with a gold-coated AFM probe tip and gold surface, there was significant improvement in the signal-to-noise ratio compared to standard IR nanospectroscopy. Also, IR difference-spectra in the 1450-1800 cm^{-1} range were collected from monolayer sample areas as thin as 10 nm with a diameter of less than 500 nm, which is far beyond the diffraction limit of traditional IR spectroscopy. With this nanoscale level of detail, there was clear spectroscopic evidence of a branching in the photocycle of BR molecules on the gold surfaces; that is, there were equal amounts of proteins either following the proton-pump photocycle or existing in an intermediate state and not contributing to the photocycle. This study serves as a model for future AFM-IR spectroscopy studies of conformational changes of proteins embedded in membranes.

Detection of a secondary structure of Alzheimer’s-related protein in water

In a study by Ramer et al., nanoscale polypeptide conformational analysis in aqueous environments was performed.⁷ Proteins typically function by folding into three-dimensional structures and binding to other molecules to form functional complexes. IR spectroscopy is well established as an important tool for chemically characterizing the secondary structure of proteins both in aqueous and solid states. However, traditional IR spectroscopy is diffraction-limited to a resolution of 3-10 μm laterally, so nanoscale protein structures previously could not have been chemically analyzed. The nanoscale chemical characterization capability of AFM-IR spectroscopy has enabled the determination of polypeptide conformations in single protein fibrils and other submicron-sized protein structures, resulting in an improved understanding of important processes as protein misfolding and aggregation mechanisms.

In this study, AFM-IR was used to probe supra-molecular aggregates of diphenylalanine, the core recognition module of the Alzheimer’s B-amyloid peptide, and its derivative Boc-diphenylalanine. With AFM-IR, the authors achieved high-resolution IR spectra and maps in air and water substrates with comparable signal-to-noise ratios, which enabled identification of chemical and structural states of

morphologically similar networks at the single aggregate level, such as fibril (Figure 2). For example, they easily collected chemical data from individual fibrils smaller than 200 nm laterally. Achieving such high resolution would not be possible with classical IR spectroscopy alone. Before this study, AFM-IR was only performed on dried materials due to concerns that the drying out of a protein-containing material could result in a conformational change in the protein backbone structure. The success of using AFM-IR for an aqueous sample here serves as proof of concept for future studies.

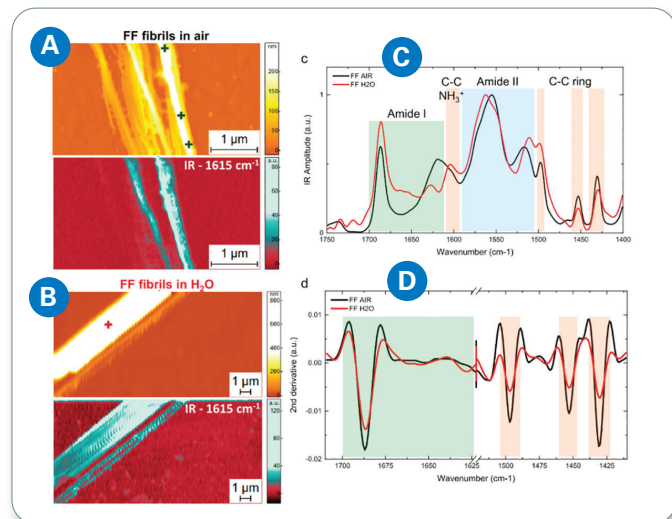


Figure 2. AFM-IR measurement of diphenylalanine (FF) fibrils in air and H₂O. morphology and IR absorption map (1615 cm⁻¹) for FF fibrils in (A) air and (B) H₂O. (C) Comparison of the average AFM-IR spectra covering the amide I band (green), amide II (blue), and C-C ring (orange) spectral regions. (D) Comparison of the second derivatives of the spectra in the amide I and C-C ring absorption. Adapted from G. Ramer, F.S. Ruggeri, A. Levin, T.P.J. Knowles, and A. Centrone, *ACS Nano* 12, 6612–6619 (2018).⁷

Phenotyping the malaria parasite during development in red blood cells

In a study by Perez-Guaita et al., multivariate image analysis was implemented to generate multivariate AFM-IR maps for collection of high-resolution, subcellular information in red blood cells infected with the malaria parasite, *Plasmodium falciparum*, at various stages in development.⁸ This approach uniquely supported the generation of compositional maps of subcellular structures in the parasites, including the food vacuole, lipid inclusions, and the nucleus, based on the intensity of hemozoin, hemoglobin, lipid, and DNA IR marker bands, respectively (Figure 3). By combining the high-resolution given by AFM-IR with hyperspectral data modeling, subcellular structures were detected directly without having to perform cell sectioning or biochemical staining. With this ability to phenotype the parasite development within red blood cells, it is possible to study the phenotypes of drug-resistant parasites and potential modes of action for antimalarial drugs.

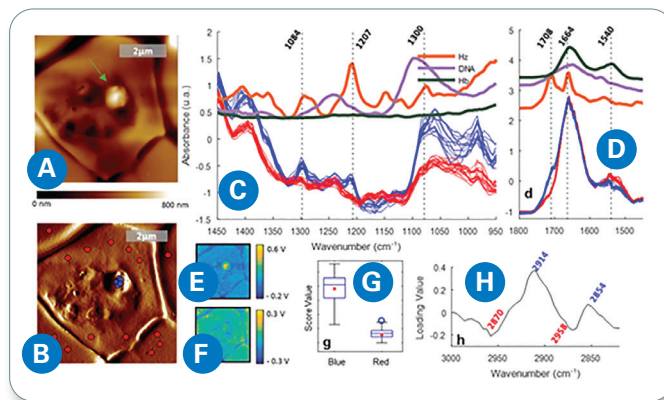


Figure 3. AFM-IR imaging of a *P. falciparum* trophozoite inside a red blood cell. (A) AFM topography. (B) AFM deflection map showing the location of the points where spectra were measured, inside (blue) and outside (red) of the protrusion. (C, D) Spectra measured from the signal of the IR intensity peak (V) showing different bands for the red and blue spots in the 1450–950 and 1800–1450 cm⁻¹ regions, respectively. (E, F) IR peak maps obtained at 1207 and 1660 cm⁻¹, respectively. (G, H) Score and loading plots from the PCA applied to the 3100–2800 cm⁻¹ region. D. Perez-Guaita, K. Kochan, M. Batty, C. Doerig, J. Garcia-Bustos, S. Espinoza, D. McNaughton, P. Heraud, and B.R. Wood. *Anal. Chem.* 90, 3140–3148 (2018).⁸

In vivo detection of molecular changes during cellular processes in bacteria

AFM-IR has been used for in vivo detection of molecular changes during cellular processes in single cells of bacteria. In a study by Kochan et al., AFM-IR spectroscopy was used to monitor nanoscale molecular changes in the cell wall during cell division in the bacteria *Staphylococcus aureus*.⁹ Dynamic changes in the cell wall during cell division in *Staphylococcus aureus* included the thickening of the septum and change in molecular components (Figure 4). The diameter of the newly forming septum was approximately 45 nm. The AFM-IR spectrum recorded from this structure clearly exhibit broadening and increased intensity of some bands (centered at 1088 and 1228 cm⁻¹ and attributed to carbohydrate and phosphodiester groups of cell-wall components), when compared with a spectrum from an area outside the septum. The second derivative of a differential spectrum, obtained by subtraction of a non-septum spectrum from the septum spectrum, exhibits bands centered at 1092 and 1240 cm⁻¹ (carbohydrate and phosphodiester modes). The chemical characterization of the septum structure at such high resolution in a live cell is uniquely possible with AFM-IR. This example demonstrates the capability of AFM-IR as a tool to gain molecular insights into cellular processes in vivo and in nanoscale detail.

In a subsequent study by Kochan et al., AFM-IR spectroscopy was combined with chemometric analysis to identify changes in the chemical composition of *Staphylococcus aureus* in relation to the development of antibiotic drug resistance to vancomycin and daptomycin at the single-cell level.¹⁰ This study focused on the use of paired clinical isolates to enable the assignment of specific

changes to the development of resistance. For vancomycin, an increase in the amount of extracellular carbohydrates was observed, indicating thickening or changes in the packing of the cell wall. By contrast, with daptomycin, an increase in phospholipid content associated with the development of nonsusceptibility was observed. This work demonstrates the potential of the AFM-IR technique for antimicrobial resistance detection at the single bacterium level.

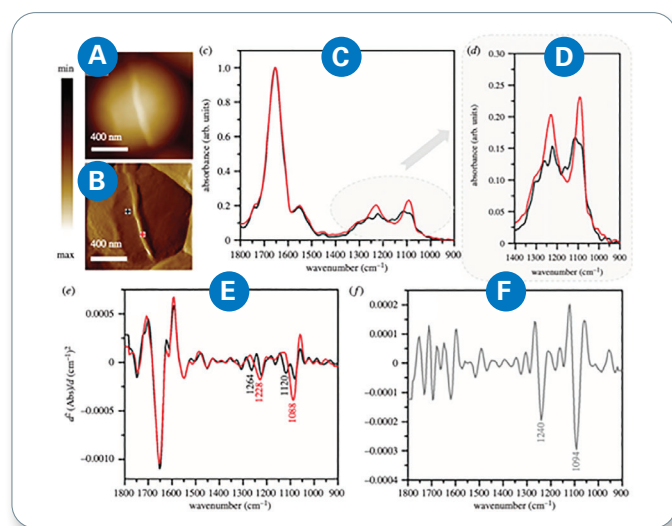


Figure 4. (A) AFM height and (B) AFM deflection image of the dividing cell collected prior to recording AFM-IR spectra at the marked points, from which spectra were recorded (non-septum in black and forming septum in red). Size of the area imaged by AFM: 1.17 1.15 μm . (C, D) Comparison of AFM-IR spectra recorded from septum (red) and non-septum (black) of the *S. aureus* cell during division in the spectral range (C) 1800–900 cm^{-1} and (D) 1400–900 cm^{-1} . Spectra were normalized to amide I band. (E) The second derivatives of spectra presented in (C), with marked prominent differentiating bands. (F) The second derivative of a differential spectrum obtained by subtraction of non-septum spectrum (C, black) from the septum spectrum (C, red), with prominent bands marked. Adapted from Kochan et al.⁹

Tracking biochemical changes in tumors in salivary gland tissue

AFM-IR has been used to define biochemical differences between healthy and tumorous salivary gland tissues. A study by Paluszkiwicz et al. was the first AFM-IR investigation of healthy salivary gland versus tumor tissue.¹¹ The use of AFM-IR uniquely allowed for the detection of fibril-like areas within the tumor tissue, with the size of one of the smallest characterized amyloid forms being 70 nm, which would be undetectable by traditional IR spectroscopy alone. The IR spectra of margin tissue (non-tumor), the areas outside of the fibrils of the tumor, and the fibril-like structure of the tumor tissue were all collected (Figure 5). With the capabilities of nanoscale IR, it was discovered that fibril-like areas within a salivary gland tumor contained higher β -sheet content, given by IR spectra, compared to regions within the tumor outside the fibrils. This level of protein secondary structure differentiation would

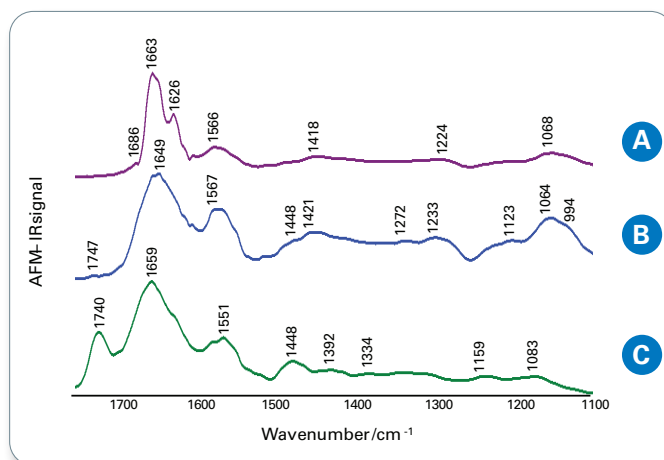


Figure 5. The averaged AFM-IR spectra of the salivary glands tissue sections in the spectral range 1800–900 cm^{-1} ; the fibril-like structure of tumor tissue (A), the areas outside the fibrils of tumor tissue (B) and the margin tissue (C).

not be possible to achieve using conventional IR or Raman microspectroscopy. The detection of biochemical differences between tumor tissue and healthy tissue may contribute to therapy progression through development of drugs with specific action informed by research.

Summary

Nanoscale IR spectroscopy can be utilized to chemically and topographically characterize nanoscale biological samples including proteins, structures within single cells, monolayers, and tissues. With photothermal AFM-IR, an IR laser irradiates the sample resulting in thermal expansion, which is detected by the AFM tip that oscillates in proportion to the thermal expansion. When a quantum cascade laser is used, it provides a signal enhancement two orders of magnitude over conventional AFM-IR spectroscopy and imaging because its repetition rate can be matched to specific mechanical resonance frequencies in the AFM cantilever. An additional two orders of magnitude improvement in sensitivity can be achieved by gold-coating the AFM tip and casting the sample films on gold substrates. It is the combination of resonance enhancement using the QCL source and the “lightning rod” effect produced by gold-coating the AFM tip and substrate that enables the detection of monolayers of material at spatial resolutions on the order of 25x25 nm. Resonance-enhanced photothermal AFM-IR is a proven useful technology for providing chemical characterization of protein films and other sample types in the life sciences, even in the presence of water. The few examples presented here demonstrate how AFM-IR is already being used to answer a variety of different biological questions. With AFM-IR, researchers have made discoveries in photocycle branching in bacteriorhodopsin molecules, secondary structures in Alzheimer’s-related proteins, phenotypes of the development of the malaria pathogen in red blood cells, in vivo detection of molecular changes during cell

processes, and biochemical changes in cancerous tissues. AFM-IR is a cutting-edge and uniquely practical technique that allows researchers to answer questions that require nanoscale-level chemical and topographical analysis of biological samples and beyond.

References

1. A. Dazzi, R. Prazeres, F. Glotin, and J.M. Ortega, *Opt. Lett.* 30, 2388-90 (2005).
2. A. Dazzi and C.B. Prater, *Chem. Rev.* 117, 5146-5173 (2017).
3. F. Lu and M.A. Belkin, *Opt. Express* 29, 19942-47 (2011).
4. F. Lu, M. Jin, and M.A. Belkin, *Nat. Photonics* 8, 307-12 (2014).
5. C. Marcott, H. Yang, C.B. Prater, and K. Kjoller, *Spectroscopy* 29(s8), 18-25 (2014).
6. V. Giliberti, R. Polito, E. Ritter, M. Broser, P. Hegemann, L. Puskar, U. Schade, L. Zanetti-Polzi, I. Daidone, S. Corni, F. Rusconi, Paolo Biagioni, L. Baldassarre, and M. Ortolani, *Nano Lett.* 19, 3104–3114 (2019).
7. G. Ramer, F.S. Ruggeri, A. Levin, T.P.J. Knowles, and A. Centrone, *ACS Nano* 12, 6612–6619 (2018).
8. D. Perez-Guaita, K. Kochan, M. Batty, C. Doerig, J. Garcia-Bustos, S. Espinoza, D. McNaughton, P. Heraud, and B.R. Wood, *Anal. Chem.* 90, 3140–3148 (2018).
9. K. Kochan, D. Perez-Guaita, J. Pissang, J.-H. Jiang, A.Y. Peleg, D. McNaughton, P. Heraud, B.R. Wood, *J. R. Soc. Interface* 15: 20180115.
10. K. Kochan, C. Nethercott, D. Perez-Guaita, J.-H. Jiang, A.Y. Peleg, B.R. Wood, and P. Heraud, *Anal. Chem.* 91, 15397–15403 (2019).
11. C. Paluszkiwicz, N. Piergies, M.C. Guidi, E. Pięta, W. Ścierański, M. Misiołek, B. Drozdowska, P. Ziara, G. Lisowska, and W. Kwiatek, *BBA - General Subjects* 1864, 129677 (2020).

Authors

Curtis Marcott, Ph.D., Senior Partner, Light Light Solutions
(marcott@lightlightsolutions.com)

Savana Lipps, Bruker Lifescience Writer
(savana.lipps@bruker.com)

Miriam Unger, Bruker Applications Scientist
(miriam.unger@bruker.com)